

CHEMISTRY

A European Journal

A Journal of



Accepted Article

Title: 5-Methylcytosine is oxidized to the natural metabolites of TET-enzymes by a biomimetic iron(IV)oxo complex

Authors: Niko S.W. Jonasson and Lena Daumann

This manuscript has been accepted after peer review and appears as an Accepted Article online prior to editing, proofing, and formal publication of the final Version of Record (VoR). This work is currently citable by using the Digital Object Identifier (DOI) given below. The VoR will be published online in Early View as soon as possible and may be different to this Accepted Article as a result of editing. Readers should obtain the VoR from the journal website shown below when it is published to ensure accuracy of information. The authors are responsible for the content of this Accepted Article.

To be cited as: *Chem. Eur. J.* 10.1002/chem.201902340

Link to VoR: <http://dx.doi.org/10.1002/chem.201902340>

Supported by
ACES

WILEY-VCH

FULL PAPER

5-Methylcytosine is oxidized to the natural metabolites of TET-enzymes by a biomimetic iron(IV)oxo complex

Niko S. W. Jonasson and Lena J. Daumann*

Abstract: Ten-eleven-translocation (TET) methyl cytosine dioxygenases play a key role in epigenetics by oxidizing the epigenetic marker 5-methyl cytosine (5mC) to 5-hydroxymethyl cytosine (5hmC), 5-formyl cytosine (5fC), and 5-carboxy cytosine (5cC). While much of the metabolism of 5mC has been studied closely, certain aspects - such as discrepancies among the observed catalytic activity of TET enzymes and calculated bond-dissociation energies of the different cytosine substrates - remain elusive. We report here that the DNA base 5mC is oxidized to 5hmC, 5fC and 5cC by a biomimetic iron(IV)-oxo complex, reminiscent of the activity of TET enzymes. Studies show that 5hmC is preferentially turned over compared to 5mC and 5fC and that this is in line with the calculated bond dissociation energies. We further report optimized syntheses of d_3 -5mC and d_2 -5hmC and in the reaction with the biomimetic iron(IV)-oxo complex these deuterated substrates showed large kinetic isotope effects, confirming the H-abstraction as the rate-limiting step. Taken together, these results shed light on the intrinsic reactivity of the C-H bonds of epigenetic markers and the contribution of the second coordination sphere in TET enzymes.

Introduction

Methylation of cytosine (C) in DNA is achieved via DNA methyl transferases (DNMTs).^[1] The hereby formed 5-methyl cytosine (5mC), an epigenetic marker, is then removed through two major pathways: active and passive demethylation. Active demethylation involves the action of TET enzymes which oxidize 5mC iteratively to 5-hydroxymethyl cytosine (5hmC)^[2,3], 5-formyl cytosine (5fC), and 5-carboxycytosine (5cC).^[4,5] Surprisingly, 5hmC is 10- and 100-fold more abundant than 5fC and 5cC, respectively.^[3,4,6] 5hmC, 5fC, and 5cC can each undergo direct demodification in which either formaldehyde, formic acid, or carbon dioxide, respectively, are formed.^[7-9] Additionally, 5fC and 5cC can be removed via the base excision repair (BER) pathway.^[5,10] The active site of TET enzymes contains an iron atom which is coordinated by the so-called facial triad: two histidine residues and a carboxylate-containing amino acid, aspartate in the case of TET2, that bind iron in a facial manner.^[11] The iron center is also coordinated by the co-factor α -ketoglutarate (α -KG), which is converted to succinate and carbon dioxide under consumption of dioxygen during the catalytic cycle (Figure 1).^[6,12] During this process, it is proposed that the iron(II) center is oxidized to iron(IV), as has been previously shown for the related taurine dioxygenases and other enzymes of the Fe/ α -KG family.^[13-15] Surprisingly, TET2 shows a substrate preference and faster turnover for 5mC, and not 5hmC/5fC, in contrast to the calculated

bond dissociation energies of the C-H bonds in these substrates.^[6] The formation rates of the active $\text{Fe}^{\text{IV}}=\text{O}$ species in the catalytic cycle were shown to be minimally affected by these respective substrates 5mC, 5hmC, or 5fC, but rather the hydrogen abstraction step during product formation. Xu and Luo have attributed this to the positioning of the substrates, in part to the distance of the abstractable hydrogen to the $\text{Fe}^{\text{IV}}=\text{O}$ center in the active site of TET enzymes. The regulation of this intricate interplay of multiple factors on the level of the catalytic domain is of particular interest to us. Iron(IV)-oxo cores as found in TET enzymes have long been explored by bioinorganic chemists.^[16-19] Pivotal for the elucidation of the mechanism of this large family of enzymes have been small-molecular-weight model complexes.^[13,20-26] Here we demonstrate that the known, water-soluble iron(IV)-oxo complex (**1**) displays activity reminiscent of TET enzymes. Studies analyzing product formation via GC-MS as well as UV-vis studies shed light on the kinetics and mechanism of the reaction of **1** with methyl cytosine and its oxidized derivatives. Further, we report straightforward and optimized syntheses of the deuterated substrates d_3 -5mC and d_2 -5hmC.

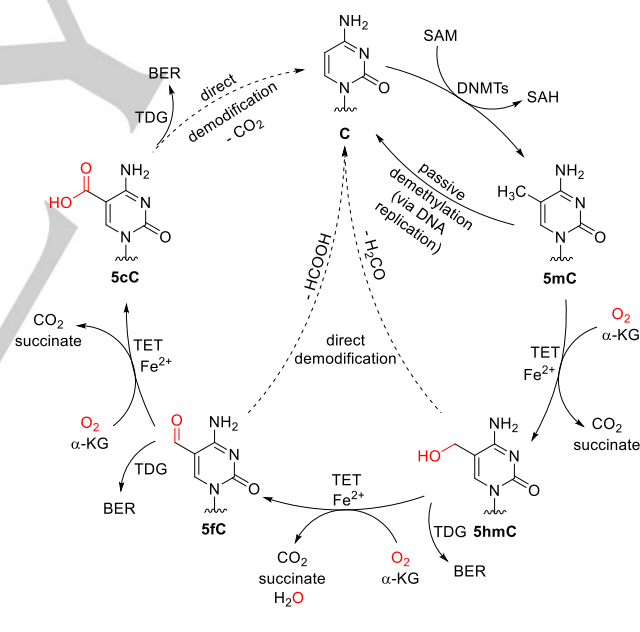


Figure 1. Proposed methylation and demethylation cycle of cytosine residues in DNA.^[7,27] The red oxygen atoms stem from molecular dioxygen that coordinates to the respective iron(II) precursor under formation of an iron(III)-superoxo intermediate, which then reacts via an iron(IV)-peroxo intermediate to the proposed active iron(IV)-oxo species under CO_2 formation.

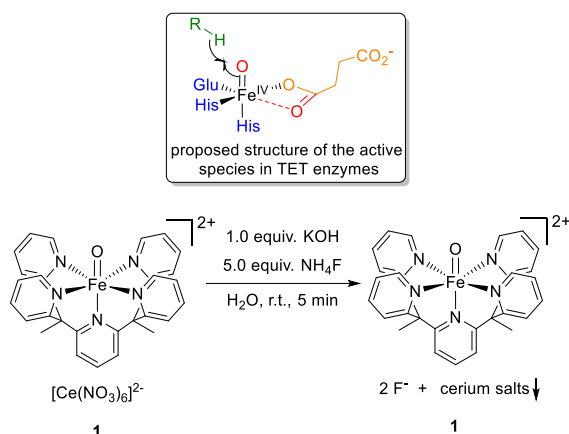
Results and Discussion

Since in the previously reported synthesis of **1**, cerium ammonium nitrate (CAN) was used as oxidant, we determined the counterion of **1**, which had not been specified previously, to be hexanitratocerate $\text{Ce}(\text{NO}_3)_6^{2-}$.^[28]

[*] N. S. W. Jonasson, Prof. Dr. L. J. Daumann
Department Chemie
Ludwig-Maximilians-University München
Butenandtstr. 5-13, Haus D
E-mail: lena.daumann@lmu.de

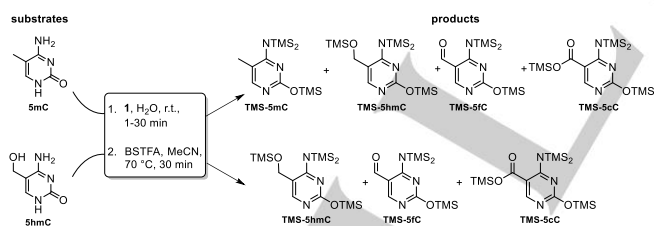
Supporting information for this article is given via a link at the end of the document.

FULL PAPER



Scheme 1. Exchange of the counterion of **1** - $[\text{Ce}(\text{NO}_3)_6]^{2-}$ (and possibly traces of other cerium salts) - by addition of potassium hydroxide and ammonium fluoride (36.9 mg **1** in 3.37 ml MilliQ, addition of 36 μl of a 1 M KOH solution and 180 μl of 1 M NH_4F solution, both in 1 M MilliQ. Removal of the cerium salts via centrifugation. For more details see supplementary information)

Inductively coupled plasma optical emission spectroscopy (ICP-OES) of $[\text{Ce}(\text{NO}_3)_6]^{2-}$ showed a ratio of 1:1 for iron and cerium, and the CHNS elemental analysis was in agreement with this composition. Unfortunately, the presence of $\text{Ce}(\text{NO}_3)_6^{2-}$ provided serious complications due to its oxidative power: hexanitratocerate is capable of oxidizing 5mC to some extent and would, therefore, interfere with our studies of the iron(IV)-oxo complex (see Figure S21). Thus we removed this counterion from **1** by addition of potassium hydroxide and ammonium fluoride for subsequent studies (Scheme 1). By systematically varying the concentrations of KOH and NH_4F , we found that 1.0 equiv. of hydroxide and 5.0 equiv. of fluoride were sufficient to achieve virtually complete removal of this counterion (Figure S32).



Scheme 2. Reaction of **1** with 5mC or 5hmC gives a product mixture that was derivatized using *N,O*-bis(trimethylsilyl)trifluoroacetamide (BSTFA) and subsequently analyzed via GC-MS (1 ml/2 ml of stock solutions (20 mM) of 5mC/5hmC, respectively, were mixed with 2 ml of a solution containing **1** (prepared as described above), 1 ml of a stock solution of U (20 mM) and 7 ml MilliQ. Samples were collected, dried, and derivatized in MeCN using BSTFA at 70 °C. For more details, see supplementary information).

As the free nucleobases represent a simplified, yet very realistic, model for epigenetically relevant DNA modifications we started our investigation of **1** with 5mC and 5hmC (Scheme 2). It

should be noted here, that many studies on iron(IV)-oxo complexes are done in non-aqueous solvents (MeCN, THF etc.) and often at very low temperatures (e.g. -40°C).^[29–31] We are reporting here a biomimetic study in water at near physiological temperature of 30°C . Using water as solvent and raising the temperature to nearly physiological values drastically improves the quality of any comparative statements that can be made about a biomimetic system. Further, less complex model substrates are often used (e.g. PPh_3 , simple olefins, alcohols or alkanes).^[28–31] **1** was previously shown by Chang *et al.* to oxidize 4-ethylbenzenesulfonate, benzyl alcohol and 4-styrenesulfonate at 25°C in water.^[28] Remarkably, with 5mC as substrate of **1** the GC-MS analysis of the TMS-derivatized mixture revealed the presence 5hmC, 5fC, and 5cC.

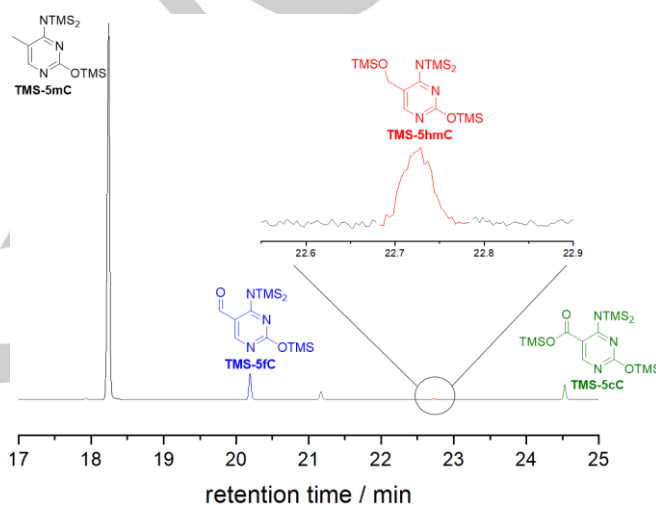


Figure 2. GC-MS traces of the TMS-derivatized product mixture collected from the reaction of 5mC with **1** as shown in Scheme 2. The small peak at $t_R = 21.17$ min was present in all measurements, for further discussion, data, and reference GC-MS traces see SI chapter 1. Control reactions involving the reaction of 5mC and/or 5hmC with air, KOH, NH_4F and $\text{NH}_4[\text{Ce}(\text{NO}_3)_6]$ were also conducted, the results can be found in the supplementary information.

Since all natural metabolites are detected in the reaction of **1** with 5mC and 5hmC, **1** can be considered a functional model for TET (Figure 2). Whereas 5fC and 5cC are detected in significant amounts, 5hmC is detected only in trace amounts. We analyzed the time-dependent product distribution by quenching a reaction of equimolar amounts of 5mC and **1** at regular time intervals (Figure 3). Use of uracil (U), which did not show any reaction with **1** (Figure S22), as an internal standard allowed us to monitor product formation trends.

FULL PAPER

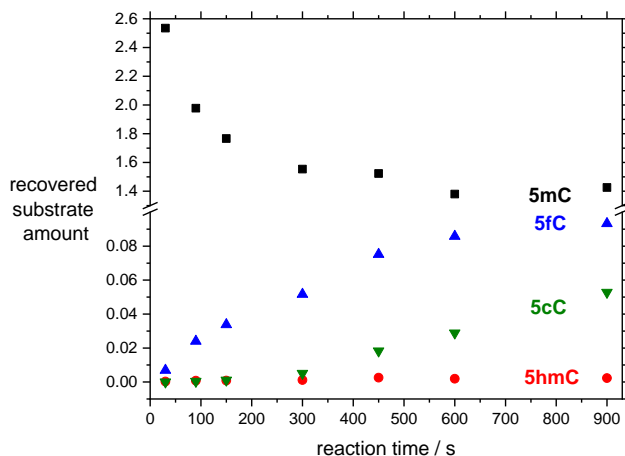


Figure 3. Trends in the recovered amounts of the silylated derivatives of 5mC, 5hmC, 5fC, 5cC present in the product mixture relative to the internal standard U as determined with GC-MS (1.0 equiv. 5mC, 1.0 equiv. U, 1.0 equiv. **1**, unbuffered water, room temperature). Note that due to the work-up the amounts of recovered starting material and products fluctuated, thus, uracil was added in a known concentration ratio regarding 5mC. The signal obtained for the derivatized uracil was set to 1 and all other signals were normalized in order to be comparable. For more information, see supplementary information.

An exponential decrease of 5mC levels was observed. 5hmC is formed during the reaction in small amounts but never reaches significant levels. We propose that the lack of significant 5hmC accumulation is due to its high reactivity towards $\text{Fe}^{\text{IV}}=\text{O}$ (without the presence of a second coordination sphere), as any 5hmC that is formed immediately reacts to 5fC. This hypothesis is further supported by our UV-vis kinetic studies (*vide infra*). 5fC is formed quickly at the beginning of the reaction and then approaches a saturation level. In addition, we studied the reaction of 5hmC with **1** under similar conditions. Due to the high reactivity of **1** towards 5hmC, the concentration of the reactants had to be reduced to 2.0 mM (from previously 10.0 mM). Under these conditions, 5fC and 5cC were detected exclusively in the product mixture (Figure S18), as expected. The high reactivity of 5hmC we noted here was a first indication for the results we obtained from our UV-vis kinetics (*vide infra*). To extract the rate laws and constants of the reaction of substituted cytosines with **1**, UV-vis spectroscopy was employed and the decrease of the $\text{Fe}^{\text{IV}}=\text{O}$ band was monitored at 718 nm. In a first set of experiments we studied the reaction of **1** with 5mC (Figure 4), the substrate concentration was varied from 0.2-1.6 equiv. at four different concentrations of **1** and *vice versa* (Figure 4A and C, respectively). A linear correlation was observed, indicating a first order behavior of both **1** and 5mC. When the linear fit slope values obtained hereby were plotted against the respective concentration of **1** or the substrate (Figures 4B and D) a linear correlation was observed. In a separate experiment, 5mC was added in excess (up to 21 equiv.) to a 1.25 mM solution of **1**. However, no saturation kinetics were observed for 5mC (see Figure S27). For 5hmC, saturation behavior was found in the concentration range used for the studies with 5mC as substrate (0.2-1.6 equiv., see Figure S30). Within the range of 0.02 to 0.16 equiv. of 5hmC, a linear behavior was observed albeit with a much steeper slope than observed for 5mC (see Figure 5).

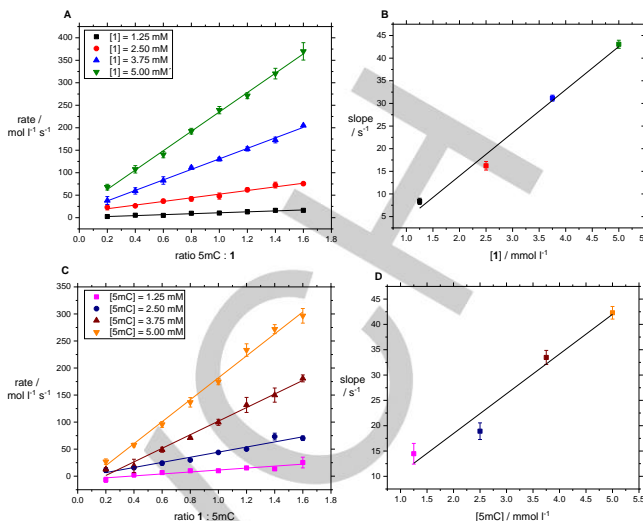


Figure 4. A: Initial rates for eight different ratios of 5mC : 1 at four different concentrations of **1** ($[\text{Fe}]$). B: Slope values of the linear fits in A plotted against their respective iron concentration. C: Initial rates for eight different ratios of 1 : 5mC at four different concentrations of 5mC. D: Slope values of the linear fits in C plotted against their respective 5mC concentration. All experiments were conducted three times and the results averaged, the error values shown represent the standard deviation. The experiments shown in Figures A and C were conducted with the two separate batches of **1** to allow for better comparability within one set of experiments. Due to the length of the experiments and slow auto-decomposition of **1**, it was not possible to conduct all experiments of A and C on the same day with the same batch of **1** (See SI).

Unfortunately, we were not able to conduct the experiment with 5mC as substrate in this low concentration range due to the slow reaction of 5mC with **1** at these concentrations resulting in large error values (Figure S28).

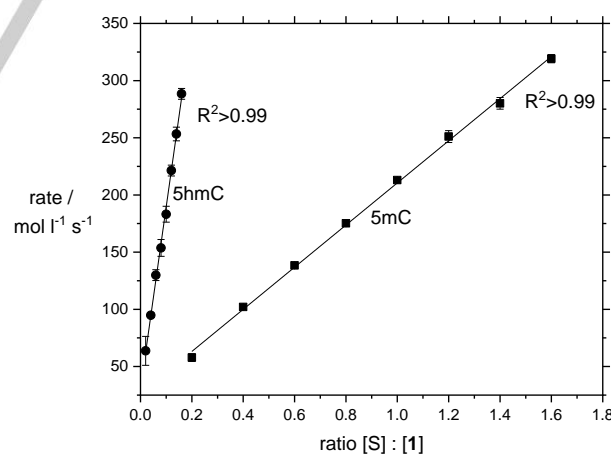


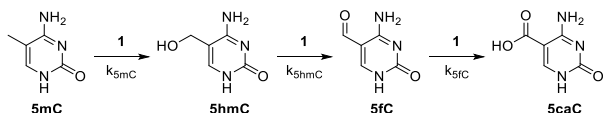
Figure 5. Initial rates for eight different ratios of 5mC:1 and 5hmC:1 in the concentration ranges 0.2-1.6 equiv. ($[\text{5mC}] = 1\text{-}8\text{ mM}$) and 0.02-0.16 equiv. ($[\text{5hmC}] = 0.1\text{-}0.8\text{ mM}$), respectively. $[\text{1}] = 5\text{ mM}$, S is either 5mC or 5hmC. All experiments were conducted with the same batch of **1** to allow for better comparability (The experiments were conducted in 96-well plate reader using 100 μl of a stock solution (10 mM) of **1** and corresponding amounts of stock solutions of 5mC and 5hmC. The overall volume was then adjusted to 200 μl , for more details, see supplementary information).

FULL PAPER

The same is true for the deuterated derivative d_2 -5hmC (see Figure S31). Also, the synthesis of 5fC and d_1 -5fC proved challenging and we were not able to obtain amounts large enough for either GC/MS or UV/Vis kinetic studies. The results presented above led us to formulate a second-order rate law for the reaction of **1** with a methylated cytosine derivative:

$$v = -k_S[1][S]$$

k_S being the rate constant with $S = 5mC, 5hmC$).



Scheme 3. Reaction of 5mC with **1** gives 5hmC, 5fC, and 5cC in a three step sequence.

From the data obtained we calculated the rate constants k_{5mC} , k_{5hmC} , k_{d_3-5mC} , and k_{d_2-5hmC} (Table 1). As mentioned before, Hu *et al.* reported rate constants for the reaction of TET2 with DNA containing 5mC, 5hmC, or 5fC and compared these values with the bond dissociation energies (BDEs) that they obtained from quantum chemical calculations.^[6] The authors noticed an unexpected trend when the substrate with the lowest BDE (5hmC) did not react the fastest, but rather 5mC did. In the case of the functional TET-model complex **1**, a clear correlation between BDE and reaction rate can be observed: 5hmC has the lowest BDE and reacts the fastest, followed by 5mC. These results highlight that, with the lack of a second coordination sphere and a hydrogen bond network, the C-H bond activation by high-valent iron(IV)oxo species follows the pattern of calculated bond dissociation energies.

Table 1. The measured rate constants k_S for the reaction of **1** with 5mC, 5hmC, and 5fC in comparison with the rate constants obtained from the reaction of **1** with the deuterated derivatives d_3 -5mC and d_2 -5hmC (concentration of **1** was always 5.0 mM) as well as the BDE calculated and the k_{cat} values determined experimentally by Hu *et al.*^[6]

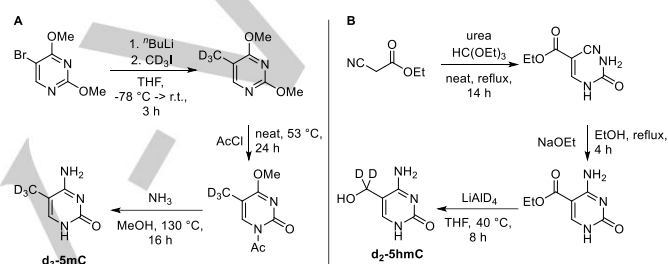
	5mC	5hmC	5fC	d_3 -5mC	d_2 -5hmC
k_S (1) [l mol ⁻¹ s ⁻¹]	7.37 ± 1.57 ^[a]	63.56 ± 12.81 ^[b]	-	0.86 ± 0.25 ^[a,c]	2.16 ± 0.52 ^[a,c]
BDE [kcal mol ⁻¹] ^[d]	90.39	86.20	92.89	-	-
k_{cat} (TET2) [10 ⁻³ s ⁻¹] ^[e]	2.12	0.63	0.46	-	-

^[a]Concentration range of substrate: 1.0-8.0 mM. ^[b]Concentration range of substrate: 0.1-0.8 mM. ^[c]Rate constants obtained from the reaction of **1** with deuterated substrates, see supplementary information Chapter 3 for detailed procedures. ^[d]As calculated by Hu *et al.* (CBS-QB3 with CPCM).^[6] ^[e]As determined experimentally by Hu *et al.*^[6]

Although we were not able to study the reaction of 5fC with **1** in detail due to the limited amount of this substrate, it seems that 5fC, which is accumulated during the reaction, does not react as quickly as 5hmC, which does not accumulate (Figure 3). It can

therefore be summarized that 5mC and 5fC react more slowly than 5hmC, which does correlate with the BDE of each substrate.

Hu *et al.* found that TET2 reacts more quickly with 5mC- than with d_3 -5mC-containing DNA albeit not reporting numbers for this kinetic isotope effect (KIE).^[6] However, their observations are in line with the results of Price *et al.* who noticed a large kinetic isotope effect (~37) for the reaction of the related TauD enzyme with (deuterated) taurine. The authors suggest that the hydrogen atom transfer (HAT) between the substrate and the iron(IV)-oxo species is the rate-limiting step.^[14,32] For model complexes, primary KIE larger than 30 have been reported.^[33,34] In order to compare the functional model to TET enzymes, we studied the reaction of **1** with the deuterated derivatives d_3 -5mC and d_2 -5hmC. These substrates were obtained in three steps from commercially available reagents using iodomethane- d_3 and lithium aluminum deuteride, respectively (see Scheme 4).



Scheme 4. A: Three step synthesis of d_3 -5mC, modified from Slatkin *et al.*,^[35] Ballweg,^[36] Wong and Fuchs,^[37] and Dvorakova *et al.*^[38] B: Synthetic sequence to obtain d_2 -5hmC, modified version of the syntheses published by Patel *et al.*^[39] In contrast to Patel *et al.*, we did not observe formation of 5cC in the reduction using LiAlH₄/LiAlD₄.

A comparison between 5mC and d_3 -5mC is shown in Figure 6, all determined rate constants can be found in Table 1.

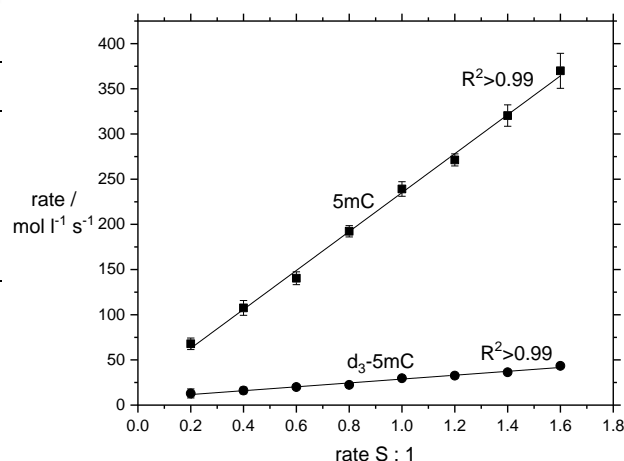
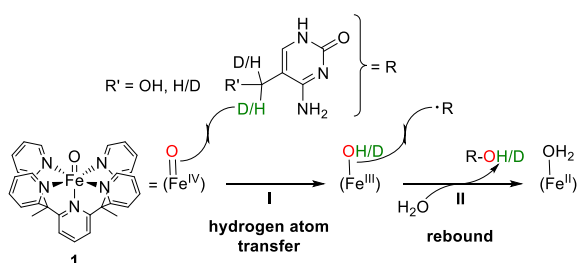


Figure 6. Comparison of the reaction rate of 5mC and d_3 -5mC, a large difference can be observed at the same ratios of S : 1 (S = 5mC, d_3 -5mC). [S] = 1-8 mM, [1] = 5 mM. All experiments were conducted with the same batch of **1** to allow for better comparability. (The experiments were conducted in 96-well plate reader using 100 μ l of a stock solution (10 mM) of **1** and corresponding

FULL PAPER

amounts of stock solutions of 5mC and d₃-5hmC. The overall volume was then adjusted to 200 µl, for more details, see SI).

These experiments show a large KIE which suggests a rate determining C-H bond cleavage for the reaction of methylated cytosine derivatives with **1** (step I in Scheme 5) opposed to a rate-limiting rebound step II. Specifically, primary KIEs >1 (~9 and 29) are observed for 5mC and 5hmC and these are well within the range of commonly observed KIEs of Fe/α-KG enzyme substrates.^[6] It is important to highlight that the rate of formation of the Fe^{IV}=O species is, here, not relevant for the C-H activation, as substrates are added to an already formed active species **1**. The Fe^{IV}=O species in enzymes is of a fleeting nature and impossible to trap at room temperature. This uncoupling of essential steps in enzyme catalytic cycles is one major advantage of biomimetic complexes.



Scheme 5. Proposed reaction mechanism of **1** with 5mC/d₃-5mC consisting of a hydrogen atom transfer from the substrate to the oxo-moiety (step I) and a rebound step in which the product is formed via a transfer of the hydroxyl group (step II).

Conclusions

In conclusion, we present here a functional model for TET enzymes connecting biomimetic Fe(IV)oxo research for the first time with epigenetics: 5mC is oxidized by the fully synthetic system **1** to the natural metabolites 5hmC, 5fC, and 5cC, as has been confirmed by GC-MS. Time-dependent measurements showed that 5hmC is formed but does not accumulate during the reaction. 5fC is formed initially and reaches a steady-state level while 5cC is formed mostly towards the end of the reaction. Exponential fits can be used to describe 5mC consumption as well as 5fC and 5cC formation. UV-vis kinetic studies complement these findings: 5hmC is observed to react the fastest by a great margin (~9 times faster than 5mC), which explains the minimal amounts detected via GC-MS in reaction of **1** with 5mC. UV-vis kinetics of deuterated substrates show a large KIE for both 5mC/d₃-5mC and 5hmC/d₂-5hmC suggesting that the hydrogen atom transfer reaction is the rate-limiting step.

The substrate preference of TET enzymes has puzzled researchers for some time.^[6] Using a known iron(IV)-oxo complex as a model for active site in TET enzymes (lacking the surrounding second coordination sphere) we were able to clearly differentiate between behavior induced via the inherent reactivity of iron(IV)-oxo moieties towards C-H bonds, and the effects of a second coordination sphere. Thus, we have demonstrated here

experimentally, that it is most likely the binding and orientation of substrate in the active site pocket in TET enzymes (not the strength of the C-H bond that is to be activated) that leads to this unusual selectivity, highlighting the absolute requirement of a second coordination sphere. In future investigations, nucleosides and nucleotides should be used as substrates, this would slowly increase the level of complexity in the substrate system in order to resemble the natural substrate, DNA, more closely, as well as a step wise incorporation of a second coordination sphere on the side of the model complex.

Experimental Section

All experimental procedures such as optimized complex and substrate syntheses as well as reaction workup procedure, GC-MS as well as UV vis kinetic protocols and NMR spectra can be found in the supporting information.

Acknowledgements

NSWJ and LJD are supported by the SFB1309 "Chemical Biology of Epigenetic Modifications" Project C5. We would like to thank Maren Haas of the research group of Prof. Oliver Trapp for her help in finding a suitable GC-MS method. Additionally, we would like to thank Eva Korytiakova of the research group of Prof. Thomas Carell for her help with HPLC separations of 5hmC and d₂-5hmC and Johann de Graaff for his preliminary investigations into the synthesis of d₃-5mC.

Keywords: 5-methyl cytosine • DNA methylation • enzyme models • TET enzymes • iron(IV)-oxo • bioinorganic chemistry

References

- [1] A. Jeltsch, R. Z. Jurkowska, *Nucleic Acids Res* **2016**, *44*, 8556–8575.
- [2] S. Kriaucionis, N. Heintz, *Science* **2009**, *324*, 929–930.
- [3] M. Tahiliani, K. P. Koh, Y. Shen, W. A. Pastor, H. Bandukwala, Y. Brudno, S. Agarwal, L. M. Iyer, D. R. Liu, L. Aravind, et al., *Science* **2009**, *324*, 930–935.
- [4] S. Ito, L. Shen, Q. Dai, S. C. Wu, L. B. Collins, J. A. Swenberg, C. He, Y. Zhang, *Science* **2011**, *333*, 1300–1303.
- [5] Y.-F. He, B.-Z. Li, Z. Li, P. Liu, Y. Wang, Q. Tang, J. Ding, Y. Jia, Z. Chen, L. Li, et al., *Science* **2011**, *333*, 1303–1307.
- [6] L. Hu, J. Lu, J. Cheng, Q. Rao, Z. Li, H. Hou, Z. Lou, L. Zhang, W. Li, W. Gong, et al., *Nature* **2015**, *527*, 118–122.
- [7] T. Carell, M. Q. Kurz, M. Müller, M. Rossa, F. Spada, *Angew. Chem. Int. Ed.* **2017**, *57*, 4296–4312.
- [8] D. Globisch, M. Münzel, M. Müller, S. Michalakis, M. Wagner, S. Koch, T. Brückl, M. Biel, T. Carell, *PLoS One* **2010**, *5*, e15367.
- [9] S. C. Wu, Y. Zhang, *Nat. Rev. Mol. Cell Bio.* **2010**, *11*, 607–620.
- [10] A. Maiti, A. C. Drohat, *J. Biol. Chem.* **2011**, *286*, 35334–35338.
- [11] E. L. Hegg, L. Que, *Eur. J. Biochem.* **1997**, *250*, 625–629.
- [12] L. Hu, Z. Li, J. Cheng, Q. Rao, W. Gong, M. Liu, Y. G. Shi, J. Zhu, P. Wang, Y. Xu, *Cell* **2013**, *155*, 1545–1555.
- [13] J. C. Price, E. W. Barr, B. Tirupati, Bollinger J. Martin, C. Krebs, *Biochemistry* **2003**, *42*, 7497–7508.
- [14] P. J. Riggs-Gelasco, J. C. Price, R. B. Guyer, J. H. Brehm, E. W. Barr, Bollinger J. Martin, C. Krebs, *J. Am. Chem. Soc.* **2004**, *126*, 8108–8109.
- [15] M. L. Neidig, C. D. Brown, K. M. Light, D. G. Fujimori, E. M. Nolan, J. C. Price, E. W. Barr, Bollinger J. Martin, C. Krebs, C. T. Walsh, et al., *J. Am. Chem. Soc.* **2007**, *129*, 14224–14231.
- [16] M. Costas, K. Chen, L. Que, *Coord. Chem. Rev.* **2000**, *200–202*, 517–544.
- [17] A. R. McDonald, L. Que, *Coord. Chem. Rev.* **2013**, *257*, 414–428.
- [18] J. E. M. N. Klein, L. Que, in *Encyclopedia of Inorganic and Bioinorganic Chemistry*, American Cancer Society, **2016**, pp. 1–22.

FULL PAPER

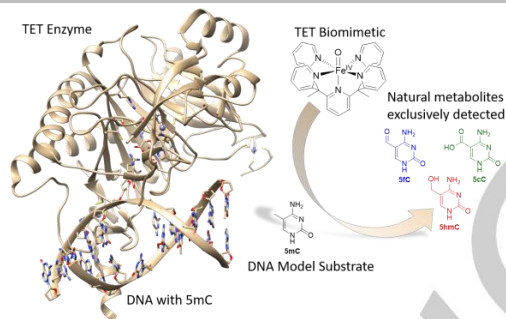
- [19] S. Kal, L. Que, *J. Biol. Inorg. Chem.* **2017**, *22*, 339–365.
- [20] C. Kim, K. Chen, J. Kim, L. Que, *J. Am. Chem. Soc.* **1997**, *119*, 5964–5965.
- [21] P. A. MacFaul, K. U. Ingold, D. D. M. Wayner, L. Que, *J. Am. Chem. Soc.* **1997**, *119*, 10594–10598.
- [22] M. H. Lim, J.-U. Rohde, A. Stubna, M. R. Bukowski, M. Costas, R. Y. N. Ho, E. Münck, W. Nam, L. Que, *PNAS* **2003**, *100*, 3665–3670.
- [23] J.-U. Rohde, J.-H. In, M. H. Lim, W. W. Brennessel, M. R. Bukowski, A. Stubna, E. Münck, W. Nam, L. Que, *Science* **2003**, *299*, 1037–1039.
- [24] J.-U. Rohde, S. Torelli, X. Shan, M. H. Lim, E. J. Klinker, J. Kaizer, K. Chen, W. Nam, L. Que, *J. Am. Chem. Soc.* **2004**, *126*, 16750–16761.
- [25] J. Bautz, M. R. Bukowski, M. Kerscher, A. Stubna, P. Comba, A. Lienke, E. Münck, L. Que, *Angew. Chem. Int. Ed.* **2006**, *45*, 5681–5684.
- [26] M. J. Collins, K. Ray, L. Que, *Inorg. Chem.* **2006**, *45*, 8009–8011.
- [27] K. Iwan, R. Rahimoff, A. Kirchner, F. Spada, A. S. Schröder, O. Kosmatchev, S. Ferizaj, J. Steinbacher, E. Parsa, M. Müller, et al., *Nat. Chem. Biol.* **2018**, *14*, 72–78.
- [28] T. Chantarojsiri, Y. Sun, J. R. Long, C. J. Chang, *Inorg. Chem.* **2015**, *54*, 5879–5887.
- [29] A. N. Biswas, M. Puri, K. K. Meier, W. N. Oloo, G. T. Rohde, E. L. Bominaar, E. Münck, L. Que, *J. Am. Chem. Soc.* **2015**, *137*, 2428–2431.
- [30] M. Puri, L. Que, *Acc. Chem. Res.* **2015**, *48*, 2443–2452.
- [31] P. Comba, S. Fukuzumi, C. Koke, B. Martin, A.-M. Löhr, J. Straub, *Angew. Chem. Int. Ed.* **2016**, *55*, 11129–11133.
- [32] J. C. Price, E. W. Barr, T. E. Glass, C. Krebs, J. M. Bollinger, *J. Am. Chem. Soc.* **2003**, *125*, 13008–13009.
- [33] J. Kaizer, E. J. Klinker, N. Y. Oh, J.-U. Rohde, W. J. Song, A. Stubna, J. Kim, E. Münck, W. Nam, L. Que, *J. Am. Chem. Soc.* **2004**, *126*, 472–473.
- [34] E. J. Klinker, S. Shaik, H. Hirao, L. Que, *Angew. Chem. Int. Ed.* **2009**, *48*, 1291–1295.
- [35] C.-Y. Shiue, A. P. Wolf, D. N. Slatkin, *J. Label. Compd. Rad.* **1980**, *17*, 177–184.
- [36] H. Ballweg, *Tetrahedron Letters* **1968**, *9*, 2171–2173.
- [37] J. L. Wong, D. S. Fuchs, *J. Org. Chem.* **1970**, *35*, 3786–3791.
- [38] A. Holý, I. Rosenberg, H. Dvořáková, *Collect. Czech. Chem. Commun.* **1989**, *54*, 2190–2210.
- [39] J. P. Patel, M. L. Sowers, J. L. Herring, J. A. Theruvathu, M. R. Emmett, B. E. Hawkins, K. Zhang, D. S. DeWitt, D. S. Prough, L. C. Sowers, *Chem. Res. Toxicol.* **2015**, *28*, 2352–2363.

FULL PAPER

Entry for the Table of Contents

FULL PAPER

5mC is oxidized by a biomimetic complex to the natural metabolites 5hmC, 5fC, and 5cC. Kinetic studies with deuterated substrates show a large KIE for both 5mC/d₃-5mC and 5hmC/d₂-5hmC suggesting a hydrogen atom transfer as rate limiting step.



Niko S. W. Jonasson and Lena J. Daumann

Page No. – Page No.
5-Methylcytosine is oxidized to the natural metabolites of TET-enzymes by a biomimetic iron(IV)oxo complex